nature geoscience

LETTERS

PUBLISHED ONLINE: 11 AUGUST 2013 | DOI: 10.1038/NGEO1895

The legacy of the Pleistocene megafauna extinctions on nutrient availability in Amazonia

Christopher E. Doughty[1]*, Adam Wolf[2] and Yadvinder Malhi[1]

In the late Pleistocene, 97 genera of large animals went extinct, concentrated in the Americas and Australia[1]. These extinctions had significant effects on ecosystem structure[2], seed dispersal[3] and land surface albedo[4]. However, the impact of this dramatic extinction on ecosystem nutrient biogeochemistry, through the lateral transport of dung and bodies, has never been explored. Here we analyse this process using a novel mathematical framework that analyses this lateral transport as a diffusion-like process, and we demonstrate that large animals play a disproportionately large role in the horizontal transfer of nutrients across landscapes. For example, we estimate that the extinction of the Amazonian megafauna decreased the lateral flux of the limiting nutrient phosphorus by more than 98%, with similar, though less extreme, decreases in all continents outside of Africa. This resulted in strong decreases in phosphorus availability in eastern Amazonia away from fertile floodplains, a decline which may still be ongoing. The current P limitation in the Amazon basin may be partially a relic of an ecosystem without the functional connectivity it once had. We argue that the Pleistocene megafauna extinctions resulted in large and ongoing disruptions to terrestrial biogeochemical cycling at continental scales and increased nutrient heterogeneity globally.

The consequence of megafauna extinctions on nutrient budgets is of particular interest because large animals play a disproportionately important role in this translocation of nutrients because they travel farther and have longer food passage times than smaller animals[5,6] (Methods). Animals are vectors of nutrients through their dung and flesh. This movement takes two main forms: the concentration of nutrients into 'hotspots'[7,8], and diffusion, the dispersion of nutrients from regions of high nutrient concentrations to regions of low nutrient concentrations[9]. Although the bulk of research has examined the former process, there is a growing body of literature documenting animal-mediated translocation of nutrients across gradients, thus providing fertility to nutrient limited ecosystems[10,11].

There are significant challenges in extrapolating these site studies to large spatial scales (continental or global scale) and over long timescales (hundreds to thousands of years). It is an even greater challenge to apply these insights to extinct fauna, about which little is known aside from body size and distribution. However, if we consider all animal species over long time periods, we propose that animal movement begins to approximate a 'random walk', such that the horizontal flux of nutrients can be modelled as a diffusion-like process analogous to the diffusion of heat (see Supplementary Information for further justification and discussion of this approximation). To estimate the diffusivity of nutrients based on body size and distribution, we make use of a large literature on body size relationships[12] describing a wide range of animal physiology and behaviour based on size (M), such as day range (DD), metabolic rate (MR), population density (PD) and food passage time (PR). We calculate a diffusion term (Φ) for dung (see Methods and Supplementary Information for derivation and explanation of all terms) according to the following equation:

$$\Phi = (1-\epsilon) * \mathrm{MR} * \frac{\mathrm{PD}}{\alpha B} * \frac{(\mathrm{DD} * \mathrm{PR})^2}{2 * \mathrm{PR}} = \frac{0.78 * 0.05 * M^{1.17}}{\alpha B} \quad (1)$$

We calculate the overall mass-scaling coefficient for Φ to be 1.17 (Figs 1 and 2a). The scaling coefficient specifically for larger herbivores (>10 kg) is even greater at 1.41 (Supplementary Information). Because the scaling coefficients are greater than one, this means that large animals are disproportionally important in the

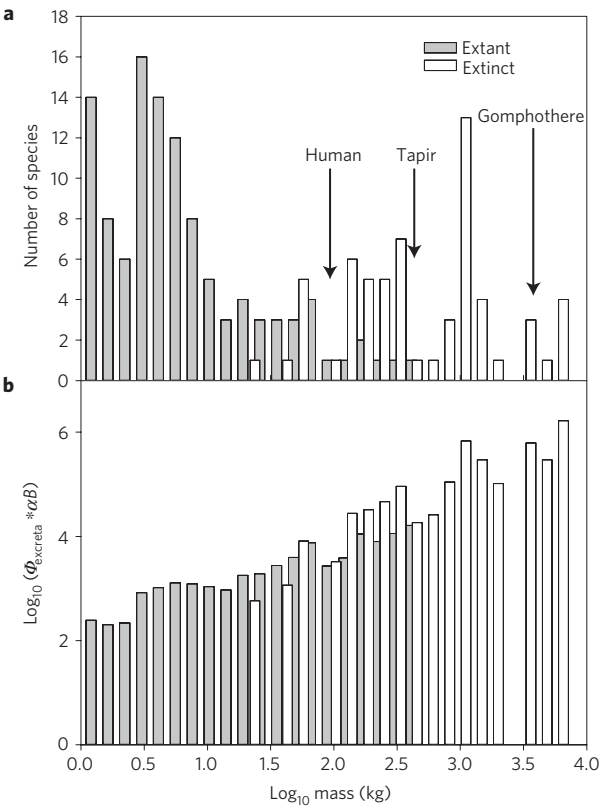

Figure 1 | Megafauna extinctions in South America and their impact on Φ. **a**, A histogram of extinct (white) and living (grey) South American fauna (>1 kg). **b**, The diffusivity term $\log_{10}$ ($\Phi_{excreta} * \alpha B$) calculated for each size class for extinct and living South American fauna (>1 kg) in units of km^2 yr^{-1}.

[1]Environmental Change Institute, School of Geography and the Environment, University of Oxford, South Parks Road, Oxford OX1 3QY, UK, [2]Department of Ecology and Evolutionary Biology, Princeton University, Princeton, New Jersey 08544, USA. *e-mail: chris.doughty@ouce.ox.ac.uk

spread of phosphorus because of their high food consumption rates, their large daily ranges, and their long gut residence times, despite their lower population density.

We next explore how the extinction of the Amazonian megafauna affected the distribution of *P* across the Amazon basin, although a very similar framework could be applied to many other potentially limiting micronutrients such as sodium, which has recently been suggested to be limiting for animals in tropical forests away from coastal regions[13]. The extinctions of the Pleistocene megafauna in South America took place over several thousand years, but were particularly concentrated following human arrival during periods of intensified climate change in South America (13,500–11,500 years ago; refs 1,14). Most known fossils of extinct megafauna have been found in regions that were known to be savannas during the Pleistocene. However, it is likely that forest-dwelling megafauna are underrepresented in the fossil record owing to the poor preservation of fossils in humid tropical forests. There is isotopic evidence that several of the extinct megafauna were browsers that would have lived in a forest environment[15]. Large body size does not preclude a forest habitat, as demonstrated by the extant forest-dwelling species of elephants, rhinos, hippos and bovids in Asia and Africa.

The extinctions in South America led to drastic changes in animal size distributions, with 70% of animal species >10 kg going extinct (62 species), including such large iconic species as gomphotheres, giant sloths and glyptodonts (Fig. 1). The mean size of animals >10 kg throughout South America dropped from 843 to 81 kg. Using our mass-scaling relationships we estimate that mean home range dropped from 61.8 to 4.8 km^2, mean day range decreased by 58%, mean food passage time decreased by 46%, mean lifetime decreased by 33% and the average distance between food consumption location and excretion location decreased by 7.0 km from 9.1 to 2.1 km. From equation (1) we estimate that the lateral nutrient transfer diffusivity Φ in the Amazon basin decreased by >98%, from ~4.4(2.4–6.5) to 0.027 $km^2\,yr^{-1}$. The extinction of the megafauna effectively 'turned off' the potential for lateral nutrient flow in terrestrial Amazonia.

We explore the consequences of this reduction of lateral nutrient transfer by modelling the phosphorus concentration *P* at a location as a function of lateral animal diffusion, input from dust deposition and *in situ* weathering, and loss to leaching. There is much evidence that phosphorus is the key limiting nutrient in many Amazonian forests. The appropriate *P* budget equation is

$$\frac{dP}{dt} = \Phi\frac{d^2P}{dx^2} - KP + G \qquad (2)$$

where *K* is a first order loss rate from phosphorus leaching and occlusion and *G* is a gain rate from dust deposition and *in situ* weathering. Dust from the Sahara is estimated to provide an average of 0.48 kg P $km^{-2}\,yr^{-1}$ to the Amazon basin[16], and we estimate *in situ* weathering rates on poor eastern Amazonian soils (Supplementary Information; ref. 17). However, a much larger source of phosphorus is contributed by the uplift of fresh bedrock from the Andes Mountains, or uplift and exposure of fertile Miocene sediments in Western Amazonia, which create a sharp boundary in fertility in Western Amazonia[18]. Andean tributaries 'whitewater rivers' deliver 806 Mg of P per year to the lowlands compared to only 43 Mg P per year for clear or black rivers[17]. This P arrives in the lowlands through flooded forests and other river estuaries which flood ~17% of the Amazon basin at the peak[19]. Consequently, vegetation growing in these whitewater floodplains has an average leaf P concentration of 1.50 mg g^{-1} ($N = 88$ tree species) versus 0.55 mg g^{-1} ($N = 220$ tree species) in *terra firme* and black water sites[20] (Supplementary Table S1).

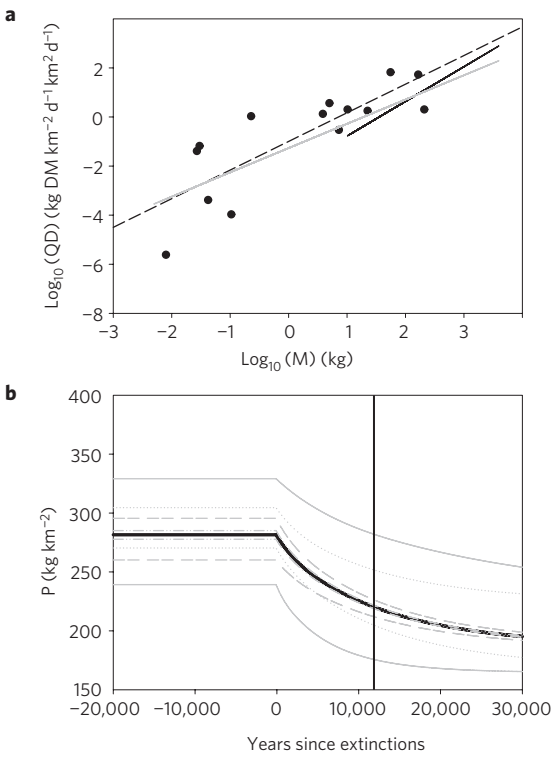

Figure 2 | Calculation of the diffusion coefficient and the impact on continental averaged South American ecosystem *P* distribution. a, Dashed line is the linear regression of $\log_{10}$ mass versus $\log_{10}$ transformed values for diffusivity (QD; kg dry matter $km^{-2}\,d^{-1} * km^2\,d^{-1}$) for all herbivores for which we have all animal values necessary (black dots) for QD ($N = 14$). Solid grey line uses the allometric equations calculated for each parameter separately and combines them to estimate QD for all herbivores and herbivores >10 kg (black line; Supplementary Information). **b**, A time series showing the step change in *P* concentrations averaged over the 2D Amazon basin simulations following extinctions 12,000 years ago. The black line is our best estimate and the grey lines are a series of sensitivity studies where we double and halve our best estimates for dust input (*G*; dotted), loss rate (*K*; solid), ε (dash dot), and $\Phi_{excreta}$ (dashed). The black vertical line indicates present day (~12,000 years following the extinctions).

This strong contrast between fertile and infertile substrates creates strong discontinuities in the supply of P (refs 20,21). The site-to-site variability in available soil P concentration is a strong determinant of vegetation P content, leading to the observation that edaphic factors control plant carbon:phosphorus ratios much more than phylogenetic factors[22]. Edaphic constraints on plant nutrient uptake in turn have strong impacts on vegetation photosynthesis, productivity, demographic rates, and biomass accumulation throughout the Amazon basin[21] in addition to species composition[18].

We solve equation (2) for *P*, with a step-change reduction in Φ at the time of the megafaunal extinction. Before the extinctions, we simulate that P was relatively well-dispersed across Amazonia, with lateral animal diffusion transporting P from the rich floodplains and western Amazonia to the much of the rest of the basin (Fig. 3a). After the extinctions, the megafauna nutrient 'pump' switched off, and this lateral transfer became much more local, and the high-phosphorus regions retreated to areas bordering the whitewater floodplains and other fertile areas (Fig. 3b,c). Even 12,000 years after the megafaunal extinction, our best estimate indicates that the Amazon basin has not yet adjusted to a post-megafaunal low nutrient steady-state—we estimate it is 67% (46–85%) of the way along the transition (Fig. 2b) (This estimate is highly dependent

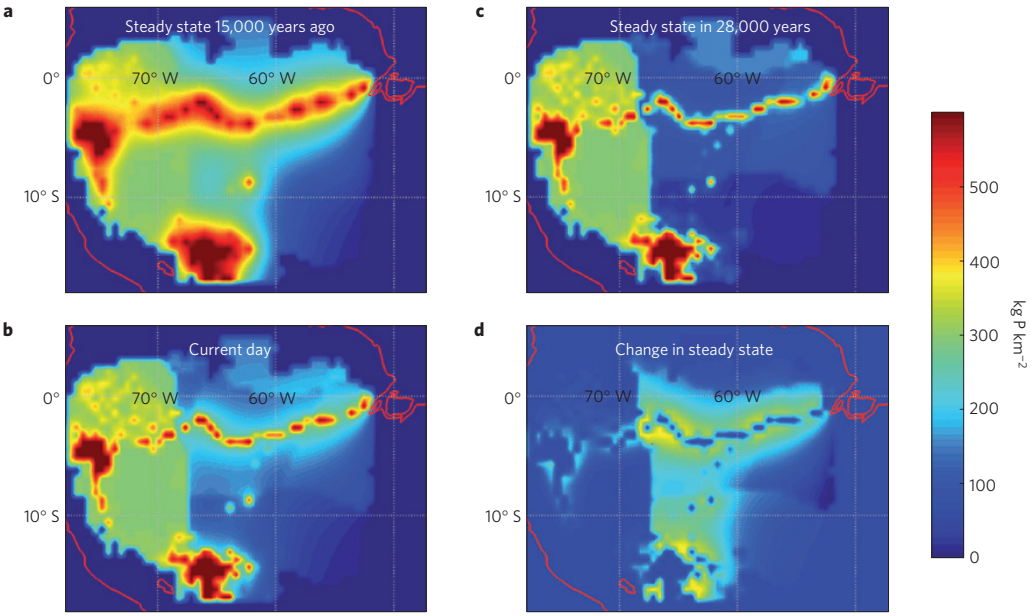

Figure 3 | Map showing changing ecosystem P concentrations in South America due to megafauna extinctions. a, The steady-state estimate of P concentrations in the Amazon basin before the megafaunal extinctions with a lateral diffusivity $\Phi_{excreta}$ value of 4.4 km^2 yr^{-1}. **b**, The current-day estimate of P concentrations 12,000 years after the extinctions with current animals and a $\Phi_{excreta}$ value of 0.027 km^2 yr^{-1}. **c**, Estimated P concentrations in the Amazon basin 28,000 years in the future. **d**, The difference between the pre- and post-extinction equilibrium (**a** and **c**).

Table 1 | Average $\Phi_{excreta} * \alpha B$ (km^2 yr^{-1}) for each continent calculated for modern species and modern plus extinct species.

	North America	South America	Australia	Eurasia	Africa
Number of species extinct	65	64	45	9	13
Mean weight of extinct animals (kg)	846	1,156	188	2,430	970
Modern $\Phi_{excreta} * \alpha B$	13,876	12,934	21,804	21,779	265,621
Modern + extinct fauna $\Phi_{excreta} * \alpha B$	140,716 (±38,000)	283,854 (±81,000)	48,250 (±8,000)	118,349 (±29,000)	324,848 (±18,000)
Percentage of original	10% (±2%)	5% (±1%)	45% (±6%)	18% (±4%)	82% (±4%)

Bottom row is the percentage of the original $\Phi_{excreta} * \alpha B$ remaining. The error represents an uncertainty in extinct species distribution of 30%.

on the loss rate (K) which is a large source of uncertainty.). Our simulated modern-day distribution of P does not include the large diversity of parent material and soil evolutionary stages which greatly impact observations of soil P across Amazonia (Supplementary Fig. S3), and instead represents the change in accessible P in the biomass-necromass-soil continuum ('ecosystem P') and not total P. Ecosystem P concentrations in intact Amazonian forests could, therefore, potentially continue to decrease (to >90% of steady state) for 17 (between 3 and 43) thousand years into the future as a legacy of the Pleistocene megafauna extinctions.

Although we have concentrated our analysis on Amazonia, it is likely that there were similar changes in nutrient transfer on all continents that experienced megafaunal extinction, albeit with variations in the local nutrient gradients and the key limiting macro- or micronutrients. Using data on Pleistocene megafaunal body masses, we estimate that Φ decreased drastically on all continents. Africa, the continent on which modern humans co-evolved with megafauna, is the only continent with most (82%) of the lateral nutrient distribution capacity still intact (Table 1). The largest declines (90–95%) were in the Americas. It seems that Eurasia also showed a large decline despite only nine extinctions, because the extinct megafauna were large (for example mammoths) whereas Australia showed a moderate decline despite a large number of extinctions, because the extinct megafauna were relatively small. However, these are estimates of non-pressured population densities, and ranges and current values for Africa and Eurasia are probably reduced owing to current pressures on megafauna, because of decreases in megafaunal population size and restrictions on their free movement across landscapes.

Following the extinction of the megafauna, humans eventually appropriated much of the net primary production that had been consumed by the extinct animals[23,24]. Did we also take over their role of nutrient dispersal? People currently provide nutrients as fertilizer to agricultural systems, but much of this gets concentrated near agriculture, suggesting that humans act as concentrating agents rather than diffusive agents like the herbivorous megafauna. Therefore, compared to earlier eras, the post-megafaunal world is characterized by greater heterogeneity in nutrient availability[25].

Our framework for estimating nutrient diffusion by animals can be applied to modern ecosystems globally, and even incorporated into global land biosphere models demonstrating the ecosystem service of nutrient dispersal. This service is analogous to that played by arteries in the human body, with large animals acting as arteries of ecosystems transporting nutrients further and smaller animals acting as capillaries distributing nutrients to smaller subsections of the ecosystem. Therefore, after the demise of its large animals, the Amazon basin has lost its nutrient 'arteries' and the widespread assumption of P limitation in the Amazon basin may be a relic of an ecosystem without the functional connectedness it once had[3]. This new mathematical framework provides a potential tool of quantifying the important but rarely recognized biogeochemical services provided by existing large animals. Therefore, those

remaining large animals under current threat in African and Asian forests can be properly valued.

More generally, we live on a planet where the nutrient supply in any one location largely reflects underlying geomorphology or abiotic input from rivers or airborne deposition (Fig. 3b,c). Our analysis suggests that this abiotic paradigm may be peculiar to a post-megafaunal extinction world. In Amazonia (and probably in many other parts of the world), we propose (and discuss methods of validation in the Supplementary Information) that large animals played a major role in diffusing nutrients across the landscape, thereby moderating the importance of local geomorphology in determining nutrient supply. To the extent humans contributed to the megafaunal extinctions, this suggests that major human impacts on global biogeochemical cycles stretch back to well before the dawn of agriculture. Aspects of the Anthropocene may have begun with the Pleistocene megafaunal extinctions.

Methods

Our mathematical derivation is presented more fully in the Supplementary Information, and the results summarized here. The equation that best incorporates the diffusive properties of animals is equation (3):

$$\frac{\partial P}{\partial t} = \Phi_{\text{excreta}} \frac{\partial^2 P}{\partial x^2} + \Phi_{\text{body}} \frac{\partial^2 P}{\partial x^2} \quad (3)$$

P is the phosphorus concentration per unit surface area, and Φ is an effective diffusivity that captures the process of nutrient consumption and defecation (Φ_{excreta}) and the process of P accumulation in bones and loss at death (Φ_{body}). In the Supplementary Information, we calculate Φ_{body} and show that it is >1,000 times smaller than Φ_{excreta}, and therefore we neglect this term in subsequent analyses. Φ_{excreta} is the product of two main terms, the lateral diffusion rate (D), which describes animal movement, and the rate of fractional consumption of edible biomass (Q). D is calculated as the limit of a random walk process[9] and is equal to $(\Delta x)^2$ (a step size in the walk) divided by $2\Delta t$ (the duration of the step). For ingestion and excretion, the step size is the mean daily displacement DD (km d^{-1}) multiplied by the average gut passage time PR (days). The timescale is the average gut passage time PR (days). To estimate the plant matter and P consumed by groups of animals, we estimate the population density of animals (PD; #/km^2) that consume dry matter (DM) to fulfill their metabolic requirements (MR; kg DM/animal/day). B represents total plant biomass (kg DM/km^2), of which α is the edible fraction. We assume αB is equivalent to foliar net primary productivity[26]. Some fraction ε of P is incorporated into the bodymass, whereas the remainder $(1-\varepsilon)$ is excreted. For megafauna, we estimate ε to be 0.22 (ref. 27; varied by $\pm$0.1 in a sensitivity study). A number of the key terms determining Φ_{excreta} are associated with body mass, including day range, DD (ref. 28), gut passage time PR (ref. 6), metabolic rate[29], and population density PD (ref. 30). The appropriate mass-scaling power-law coefficients for herbivores >10 kg are: day range 0.43; gut passage time 0.28; metabolic rate 0.87; population density −0.58. These are detailed and justified in the Supplementary Information.

Received 21 January 2013; accepted 24 June 2013; published online 11 August 2013

References

1. Barnosky, A. D., Koch, P. L., Feranec, R. S., Wing, S. L. & Shabel, A. B. Assessing the causes of Late Pleistocene extinctions on the continents. *Science* **306,** 70–75 (2004).
2. Gill, J. L., Williams, J. W., Jackson, S. T., Lininger, K. B. & Robinson, G. S. Pleistocene Megafaunal collapse, novel plant communities, and enhanced fire regimes in North America. *Science* **326,** 1100–1103 (2009).
3. Janzen, D. H. & Martin, P. S. Neotropical anachronisms—the fruits the gomphotheres ate. *Science* **215,** 19–27 (1982).
4. Doughty, C. E., Wolf, A. & Field, C. B. Biophysical feedbacks between the Pleistocene megafauna extinction and climate: The first human-induced global warming? *Geophys. Res. Lett.* **37,** L15703 (2010).
5. Kelt, D. A. & Van Vuren, D. H. The ecology and macroecology of mammalian home range area. *Am. Nat.* **157,** 637–645 (2001).
6. Demment, M. W. & Vansoest, P. J. A nutritional explanation for body-size patterns of ruminant and nonruminant herbivores. *Am. Nat.* **125,** 641–672 (1985).
7. Hutchinson, G. E. *Survey of Contemporary Knowledge of Biogeochemistry* Vol. 3 (Pemberley Books, 1950).
8. Mcnaughton, S. J. Ecology of a grazing ecosystem—the Serengeti. *Ecol. Monogr.* **55,** 259–294 (1985).
9. Okubo, A. & Levin, S. A. *Diffusion and Ecological Problems: Modern Perspectives* 2nd edn (2001).
10. Stevenson, P. R. & Guzman-Caro, D. C. Nutrient transport within and between habitats through seed dispersal processes by woolly monkeys in North–Western Amazonia. *Am. J. Primatol.* **72,** 992–1003 (2010).
11. Abbas, F. *et al.* Roe deer may markedly alter forest nitrogen and phosphorus budgets across Europe. *Oikos* (2012).
12. Peters, R. H. *The Ecological Implications of Body Size* (Cambridge Univ. Press, 1986).
13. Kaspari, M., Yanoviak, S. P. & Dudley, R. On the biogeography of salt limitation: A study of ant communities. *Proc. Natl Acad. Sci. USA* **105,** 17848–17851 (2008).
14. Barnosky, A. D. & Lindsey, E. L. Timing of Quaternary megafaunal extinction in South America in relation to human arrival and climate change. *Quat. Int.* **217,** 10–29 (2010).
15. MacFadden, B. J. Diet and habitat of toxodont megaherbivores (Mammalia, Notoungulata) from the late Quaternary of South and Central America. *Quat. Res.* **64,** 113–124 (2005).
16. Mahowald, N. M. *et al.* Impacts of biomass burning emissions and land use change on Amazonian atmospheric phosphorus cycling and deposition. *Glob. Biogeochem. Cycles* **19,** Gb4030 (2005).
17. Richey, J. E. & Victoria, R. L. in *Interactions of C, N, P, and S Biogeochemical Cycles and Global Change* (eds Mackenzie, F. T., Wollast, R. & Chou, L.) 123–140 (Springer, 1993).
18. Higgins, M. A. *et al.* Geological control of floristic composition in Amazonian forests. *J. Biogeogr.* **38,** 2136–2149 (2011).
19. Hess, L. L., Melack, J. M., Novo, E. M. L. M., Barbosa, C. C. F. & Gastil, M. Dual-season mapping of wetland inundation and vegetation for the central Amazon basin. *Remote Sens. Environ.* **87,** 404–428 (2003).
20. Furch, K. & Klinge, H. Chemical relationships between vegetation, soil and water in contrasting inundation areas of Amazonia. *Spec. Publ. Br. Ecol. Soc.* 189–204 (1989).
21. Quesada, C. A. *et al.* Variations in chemical and physical properties of Amazon forest soils in relation to their genesis. *Biogeosciences* **7,** 1515–1541 (2010).
22. Fyllas, N. M. *et al.* Basin-wide variations in foliar properties of Amazonian forest: Phylogeny, soils and climate. *Biogeosciences* **6,** 2677–2708 (2009).
23. Doughty, C. E. The development of agriculture in the Americas: An ecological perspective. *Ecosphere* **1** http://dx.doi.org/10.1890/ES10-00098.1 (2010).
24. Doughty, C. E. & Field, C. B. Agricultural net primary production in relation to that liberated by the extinction of Pleistocene mega-herbivores: an estimate of agricultural carrying capacity? *Environ. Res. Lett.* **5,** 044001 (2010).
25. Robertson, G. P. & Vitousek, P. M. Nitrogen in agriculture: Balancing the cost of an essential resource. *Annu. Rev. Env. Resour.* **34,** 97–125 (2009).
26. Mcnaughton, S. J., Oesterheld, M., Frank, D. A. & Williams, K. J. Ecosystem-level patterns of primary productivity and herbivory in terrestrial habitats. *Nature* **341,** 142–144 (1989).
27. Rees, P. A. Gross assimilation efficiency and food passage time in the African elephant. *Afr. J. Ecol.* **20,** 193–198 (1982).
28. Carbone, C., Cowlishaw, G., Isaac, N. J. B. & Rowcliffe, J. M. How far do animals go? Determinants of day range in mammals. *Am. Nat.* **165,** 290–297 (2005).
29. Kleiber, M. Body size and metabolic rate. *Physiol. Rev.* **27,** 511–541 (1947).
30. Damuth, J. Interspecific allometry of population-density in mammals and other animals—the independence of body-mass and population energy-use. *Biol. J. Linn. Soc.* **31,** 193–246 (1987).

Acknowledgements

We thank A. Barnosky and E. Gloor for comments as well as S. Levin, J. Murray and E. Lindsey for advice. C.E.D. was supported by the Gordon and Betty Moore Foundation and Geocarbon. A.W. is supported by the Carbon Mitigation Initiative of the Princeton Environmental Institute. Y.M. is supported by the Jackson Foundation and an ERC Advanced Investigator grant.

Author contributions

C.E.D. developed the original idea of the paper. C.E.D., Y.M. and A.W. developed the mathematical framework and C.E.D. and A.W. ran the models. C.E.D. led the writing of the paper with contributions from Y.M. and A.W.

Additional information

Supplementary information is available in the online version of the paper. Reprints and permissions information is available online at www.nature.com/reprints. Correspondence and requests for materials should be addressed to C.E.D.

Competing financial interests

The authors declare no competing financial interests.

nature geoscience

SUPPLEMENTARY INFORMATION

DOI: 10.1038/NGEO1895

The legacy of the Pleistocene megafaunal extinctions on nutrient availability in Amazonia

Table of contents

Overview pg 2

Justification for the random walk pg 3

Estimate of $D_{excrement}$ and D_{body} pg 5

Consumption of nutrients pg 6

Estimates of coefficients for D pg 9

1D solution pg 10

2D solution pg 12

Continental scale analysis pg 16

Possibilities to test predictions pg 17

Tables pg 19

Figures pg 21

References pg 24

17

18 Overview

19 In this paper, our goal is to estimate diffusive lateral nutrient fluxes by herbivores. In diffusion,
20 the flux is proportional to the local concentration difference in material, with a constant of proportionality
21 termed the "diffusivity" D (length^2/time). The equation that best incorporates the diffusive properties of
22 animals is the following reaction diffusion equation:

23 $$\frac{dP}{dt} = D\frac{\partial^2 P}{\partial x^2} - KP + G \qquad [1]$$

24 where K is a first order loss rate and G is a gain rate. To calculate a diffusion term we estimate D based
25 on the random walk with the form:

26 $$D = \frac{(\Delta x)^2}{2\Delta t} \qquad [2]$$

27 Where Δx is a change in distance and Δt is a timestep of duration t. In general, a diffusivity can be
28 derived from a random walk [1-3]. The "random walk" has been derived previously [4].

29

30

31

Justification for the random walk

Individual animals do not move randomly, but the net movement of all animals over long time periods (>1000 years) begins to approximate random motion. There is a large literature describing how different animal species overlap in space by consuming different foods and moving and sleeping in different patterns to avoid a variety of predators[5-7]. Internal demographics of animal groups will also change which will lead to shifting ranges and boundaries of the group over time [8].

Next, large herbivores patterns will change in response to changing climate. For instance, herbivores often track landscape patterns in grass productivity [9] which will change in response to variable rainfall patterns[10], which have experienced large global shifts over the past 15,000 years. Such interannual variation in climate alters the productivity of the landscape, which drives changes in animal foraging intensity [11,12]. These shifting patterns will serve to further move herbivore patterns from their current routes. For instance, in Kenya, during wet years there is a net nutrient input into certain patches because the impala dominate, but in dry years there may be a net loss, because the cattle dominate[13]. Due to these reasons, the net movement of all animals over long periods will approach an approximation of randomness.

As long as there is an underlying substrate concentration gradient, over long periods of time if the net movement is approximately random, animals will move the nutrients across the gradient. This seems to contradict literature showing that megafauna concentrate nutrients in small scale patches [13]. However, there is no contradiction, only a difference in the time, distance, and lack of a substrate concentration gradient. The study on megafaunal nutrient concentration focused on small nutrient patches in central Kenya (~1ha nutrient rich vegetation per 1km^2 nutrient poor vegetation) within homogenous nutrient poor metamorphic soil substrate. To the north of that study sites are rich basaltic soils of N. Kenya and Ethiopia. As these small patches of nutrient concentration shift across the landscape on decadal and larger timescales, nutrients will flow from the nutrient rich basalt to the nutrient poor metamorphic substrate

from patch to patch, through the large herbivores, over hundreds of km's and thousands of years. We have used our model to show a similar process for Kruger Park between nutrient rich basalts and granites in a companion paper[14].

There is evidence that the small scale nutrient hotspots shown in the Augustine et al. 2003 paper will shift with time. That paper depicts the creation of nutrient hotspots by the corralling of cattle where significant quantities of dung accumulate over time[13]. They then measure a significant decline in the nutrients of these areas as they are abandoned over time. It is unlikely that these nutrients are lost but instead redistributed, thus showing how nutrient hotspots can build up but then move over short time periods (~40 years).

This process has also been experimentally demonstrated in a recent study where the authors measured the total seed biomass transported between the white water floodplains and the terra firme forests by a population of wooly monkeys. They show that a single, relatively small species can transport phosphorus in quantities similar to that arriving from atmospheric deposition[15]. There was no net movement of seed biomass between the two regions, but P was transported between the sites only due to the nutrient concentration gradient. There are several other similar studies showing the net movement of nutrients by animals [16,17]. Our mathematical framework enables us to estimate this process over all animals and long periods of time.

Estimate of $D_{excreta}$

Nutrients can be moved by animals through either their dung or flesh. Nutrients moved in dung will have different distance and time scales than those moved in the flesh. We therefore calculate D for each separately. Below we start with D for dung.

Δx is the daily displacement or day range (DD) of a single animal (DD; km), and Δt is a day. The length scale for diffusivity of ingestion and excretion is the day range multiplied by the average gut passage time (PT; fractions of a day). The time scale is again the food passage time (PT). Therefore, putting this in the framework of the random walk, we estimate that the diffusivity for transport of its dung is $D_{exreta} \sim= (DD*PT)^2/(2*PT)$, where the numerator is in km^2 and the denominator is in days.

Estimate of D_{body}

Next, we calculate a D term for nutrients incorporated into the animal's body. The diffusivity for nutrients in an animal's bodymass, D_{bones}, is related to the lifetime of the animal L (days) and the residence time of these nutrients is L. The length scale is the home range (HR; km^2). The mean displacement over the lifetime of an animal is related to the range length (RL) and approximately $HR^{0.5}/2\pi$. Therefore, if HR is the range used throughout an animal's lifetime, then $D_{body} \sim= RL^2/2L$ or $HR/(8\pi^2 L)$, where the numerator is in km^2 and the denominator is in days.

Consumption of nutrients

Next, we need to estimate the amount of food and nutrients consumed by a population of animals per area. P(x,t) is the mass (kg P km^{-2}) of a nutrient. The mass of P at position x at time t+Δt is given by:

$$P(x,t+\Delta t) = P(x,t) - losses + gains \quad [3]$$

The *losses* term is represented in Equation 3 by αp(x,t), the fraction of animals leaving x at time t. The loss of a nutrient in dry matter consumed and transported by a population of animals is

$$\alpha \frac{animals}{km^2} \frac{kgDM/\Delta t}{animal} \frac{kgP}{kgDM}(x,t)\Delta t = \alpha \cdot PD \cdot MR \cdot [P](x,t)\Delta t = \alpha Q[P](x,t)\Delta t \quad [4]$$

The loss rate of P (kg DM km^{-2}) is the population density of animals (PD; #/km^2) consuming dry matter (DM) to fulfil their metabolic requirements (MR; kg DM/animal/day). The product of PD and MR is the population consumption rate of DM (denoted Q here), such that QΔt is the mass of DM consumed in Δt (kg DM km^{-2}). The consumption of the nutrient itself is then determined by Q[P](x,t), which has units kg P km^{-2}, equivalent to P, the numerator on the left. Gains from adjacent regions will be represented as Q[P](x+Δx, t) and Q[P](x-Δx, t). A fraction ε of the consumed nutrient is incorporated into bodymass, while the rest (1-ε) is excreted.

We estimate ε as 22.4% for megafauna based on the gross food assimilation efficiency of elephants [18]. Incorporation of phosphorus into the body is, of course, more complicated with relative P fraction of biomass increasing with size due to the greater investment in bone growth in larger vertebrates [19]. It also changes with animal age as full grown adult vertebrates need less P than immature growing animals. However, since we account for both the fraction in the biomass and the fraction excreted and there are no fates of the nutrient other than bodymass or excrement, we use the simple value of 22.4%.

120 To account for the large uncertainty in this term, in a sensitivity study we increase and decrease it by 0.1
121 (12.4% and 32.4%).

122 Consider the budget of just the fraction (1-ε) of consumed nutrient that will be excreted:

123 $$P(x,t+\Delta t) = P(x,t) - (1-\varepsilon)\left[\alpha Q[P](x,t) + \frac{\alpha}{2} Q[P](x+\Delta x,t) + \frac{\alpha}{2} Q[P](x-\Delta x,t) \right] \quad [5]$$

124 By analogy to the derivation the random walk, we arrive at the equation:

125 $$\frac{\partial P}{\partial t} = (1-\varepsilon) Q D_{excreta} \frac{\partial^2 [P]}{\partial x^2} \quad [6]$$

126 Adding in the fraction of nutrient incorporated into bodymass we get the complete budget equation:

127 $$\frac{\partial P}{\partial t} = (1-\varepsilon) Q D_{excreta} \frac{\partial^2 [P]}{\partial x^2} + \varepsilon Q D_{body} \frac{\partial^2 [P]}{\partial x^2} \quad [7]$$

128 The state variable on the left and the right are not the same; P is per area and [P] is per kg DM. Let B be
129 total plant biomass (kg DM km^{-2}) such that [P]B=P. We note that B has the same units as Q. Dividing
130 both sides by B:

131 $$\frac{\partial [P]}{\partial t} = (1-\varepsilon) \frac{Q}{B} D_{excreta} \frac{\partial^2 [P]}{\partial x^2} + \varepsilon \frac{Q}{B} D_{body} \frac{\partial^2 [P]}{\partial x^2} \quad [8]$$

132 B represents total plant biomass but animal consumption is only from edible parts of that biomass.
133 Therefore B' = αB, where α is the edible fraction of total biomass. We assume for simplicity here that all
134 P made available is taken up, on a fast timescale and used in edible parts. We may revisit this assumption
135 in future work. If these fractions can be assumed equal, then:

136 $$\frac{\partial [P]}{\partial t} = (1-\varepsilon) \frac{Q}{\alpha B} D_{excreta} \frac{\partial^2 [P]}{\partial x^2} + \varepsilon \frac{Q}{\alpha B} D_{body} \frac{\partial^2 [P]}{\partial x^2} \quad [9]$$

137 If Q/B can be assumed constant, then:

138 $$\frac{\partial P}{\partial t} = \Phi_{excreta} \frac{\partial^2 P}{\partial x^2} + \Phi_{body} \frac{\partial^2 P}{\partial x^2} \quad [10]$$

139 where the [P] terms on both sides have been multiplied by αB, and

140 $$\Phi_{excreta} = (1-\varepsilon)\frac{Q}{\alpha B} D \ = (1-\varepsilon)\frac{PD}{\alpha B} * MR * \frac{(DD * PR)^2}{2 * PR} \quad [11]$$

141 $$\Phi_{body} = \varepsilon \frac{Q}{\alpha B} D = \varepsilon \frac{PD}{\alpha B} * MR * \frac{HR}{8\pi^2 L} \quad [12]$$

142 We solve the equations above using datasets and methods described in the next section.

143

144 *Coefficients for* Φ *from data*

145 We compiled data for as many herbivore species as we could find for weight, day range, home
146 range, lifetime, population density, and metabolic rate. We used a common taxonomic authority [20],
147 available online at http://www.bucknell.edu/msw3/export.asp. We compiled data for terrestrial mammals
148 at the species level (n = 5278 unique taxa) but only used herbivores in our calculations. We collected
149 data for longevity and metabolic rate from the AnAge database [21]; population density [22]; day range [23]; and
150 home range [24], which all include M as a predictor variable, as well as M [25]. We use the equation from [26]
151 for food passage time. Each scaling term is not perfect but will approximate the "average" animal well
152 which is important for our study because we incorporate all animals in the ecosystem. Certain terms,
153 such as that for population density[27], are also more controversial than others, but even population density
154 shows a strong relationship with mass for large animals (although not for smaller animal).

155 We estimated Φ as a function of M in two ways: first, we calculated the allometries for each term
156 as a function of M (using ordinary least squares) and combined the resulting coefficients to yield an
157 allometric equation for Φ that results from scaling arguments (SOM Figure 1 and SOM Table 2). For
158 example, to calculate the grey and black lines for QD_{scaled} in Figure 2a, we calculated the allometries for
159 each attribute and combine them (SOM Figure 1 for herbivores >10kg). Second, we multiplied the terms
160 together to estimate Φ directly, and fit the allometric equation using the data themselves (Figure 2a). In
161 Figure 2, we were able to calculate QD_{fit} for the following fourteen species: *Eulemur fulvus*, *Propithecus*
162 *verreauxi*, *Alouatta palliata*, *Cercopithecus mitis*, *Colobus guereza*, *Dipodomys merriami*, *Perognathus*
163 *longimembris*, *Apodemus flavicollis*, *Apodemus sylvaticus*, *Rattus rattus*, *Capreolus capreolus*,
164 *Odocoileus virginianus*, *Cervus elaphus*, *Kobus ellipsiprymnus*.

165

166

167 *1D solution*

168 Below is the solution for equation 1 in 1 dimension:

169 An ordinary differential equation for a nutrient with exogenous gains G (kg P km^{-2} day^{-1}) and first

170 order losses K (day^{-1}) has the following form:

171 $$\frac{dP}{dt} = -KP + G \qquad [13]$$

172 The steady state P_{ss} of this system is G/K. We then add the diffusion term Φ which adds the potential for

173 lateral fluxes to emerge from horizontal gradients in P:

174 $$\frac{dP}{dt} = \Phi\frac{d^2P}{dx^2} - KP + G \qquad [14]$$

175 We make the following two substitutions, u = KP – G and $v = ue^{kt}$, to get the homogeneous equation

176 $$\frac{dv}{dt} = \Phi\frac{d^2v}{dx^2} \qquad [15]$$

177 We assume a boundary condition with one edge (x=0) with a fixed concentration of a nutrient that is

178 continuously replenished. Crank [28] presented the following solution. Let a line source of material have

179 concentration vo within a domain of width dξ, such that its initial mass is $v_o d\xi$. The general solution for

180 this line source, if diffusion is only in the +x direction, is

181 $$v(\xi,t) = \frac{v_o d\xi}{\sqrt{\pi D t}}\exp\left(\frac{-\xi^2}{4\Phi t}\right) \qquad [16]$$

182 Integrating this expression over dξ yields:

183 $$v(x,t) = \frac{v_o}{\sqrt{\pi\Phi t}}\int_x^\infty \exp\left(\frac{-\xi^2}{4\Phi t}\right)d\xi = v_o\frac{2}{\sqrt{\pi}}\int_{x/\sqrt{4\Phi t}}^\infty \exp(-\eta^2)d\eta \qquad [17]$$

184 where $\eta=\xi/\sqrt{4\Phi t}$. In evaluating the integral, consider the error function

185 $$erf(z) = \frac{2}{\sqrt{\pi}}\int_0^z \exp(-\eta^2)d\eta \qquad [18]$$

where erf(∞) = 1 and erf(0) = 0, and the error function complement erfc(z) = 1-erf(z). The integral then equals

$$\frac{2}{\sqrt{\pi}}\int_{x/\sqrt{4\Phi t}}^{\infty}\exp(-\eta^2)d\eta=\frac{2}{\sqrt{\pi}}\int_{0}^{\infty}\exp(-\eta^2)d\eta-\frac{2}{\sqrt{\pi}}\int_{0}^{x/\sqrt{4\Phi t}}\exp(-\eta^2)d\eta \qquad [19]$$

yielding the solution

$$v(x,t)=v_o erfc(\frac{x}{\sqrt{4\Phi t}}) \qquad [20]$$

By the previous substitutions, $v_o = e^{kt}(KP_o - G)$, where P_o is the nutrient concentration at the x=0 boundary. Backsubstituting $P(x,t) = (v(x,t)e^{-kt}+G)/K$, the solution in conventional units is:

$$P(x,t)=\left(P_o-G/K\right)erfc\left(\frac{x}{\sqrt{4\Phi t}}\right)+\frac{G}{K} \qquad [21]$$

We use equation 21 to calculate SOM figure 2. We estimate G as 0.48kg P km^{-2} yr^{-1}[29] , and local weathering at 2.5kg P km^{-2} yr^{-1} (see below), for a G of 2.98 kg P km^{-2} yr^{-1} , K as 0.00007 yr^{-1} [30], and P_o as 600 kg km^{-2} (SOM Table 2). These figures show the distribution over time from a starting point for current fauna of $\Phi_{excreta}$ =0.027 km^2 yr^{-1} (SOM figure 2 bottom) and then including the extinct megafauna $\Phi_{excreta}$ = 4.4 km^2 yr^{-1} (SOM figure 2 top).

2D solution

We could not solve equation 1 directly for a 2D scenario and we therefore use the Crank-Nicolson method to numerically solve equation 1 at each pixel at a time step of 10 years [31]. We estimate flooded white water pixels using a map of flooded areas from Hess et al. (2002) calculated using synthetic aperture radar at 30 meter resolution [32]. We then separate nutrient rich white water rivers (including the Ucayali, Maranon, Napo, Caqueta, and Madeira) from nutrient poor black and clear water rivers according to figure 1 in McClain et al. (2008) [33]. We estimate that vegetation growing in the whitewater floodplain have an average leaf P concentration of 1.50 mg g^{-1} which is continuously replenished (600 kg P km^{-2} assuming an average LAI of 4, and a SLA of 100g m^{-2}) (SI Table 1)[34]. We assume an efficient transfer of the phosphorus from the herbivore dung to the edible biota because nutrients, especially P, recycle rapidly and efficiently in tropical forests [35].

We estimate the spatial distribution of dust into the Amazon basin based on figure 8a from Mahowald et al. 2005 [29]. In a sensitivity study we double and halve these numbers due to uncertainty on how these numbers may have varied in the past (i.e. such as due to changes in the jet stream). We estimate soil moisture in the Amazon basin showing a gradual drying from the northwest to the southeast and soil moisture changing from 0.6 to 0.5 m^3 m^{-3} along this gradient. We map higher P concentrations in the more fertile western region following Higgins et al. (2011) figure 3 top [36]. This increased fertility is probably related to the removal of cation-poor surface sediments through river movement which exposes cation-rich sediments from the Pebas formation [36]. We estimate that vegetation in this region has a continually replenished source of 300 kg P km^{-2}. There is very little data on average local weathering rates in the central and eastern Amazon. However, the ratio of P carried by whitewater rivers to the more numerous black and clear water rivers is 806 Mg P versus 43 Mg P. The area of black and clear water rivers are ~3 times greater than white water rivers [33] and the P from black and clear water rivers is from local weathering, dust, and herbivore input. Therefore, we roughly assume the highly weathered Eastern

lowland soils have a local weathering rate of ~2.5 kg P km^{-2}, which we double and halve in a sensitivity study [37]. In addition, if we assume the long term steady state P (G/K) equals the labile P pool, with a median value of ~50Mg km^{-2} in the Eastern Amazon (see below)[38], a loss rate of 0.00007 yr^{-1}(see below) [30], and average dust input of 0.48kg km^{-2} [29], then to achieve steady state, there must be an additional ~2.5 kg P km^{-2} which we attribute to local weathering.

We estimate P losses from the system based on the following equations from Buendia et al. 2010 [30]:

$$LQ(s) = k_l s^c \quad [22]$$

$$L_o = k_r * LQ(s) * P_o \quad [23]$$

$$L_d = LQ(s) * \frac{Pd}{n * Zr * s} \quad [24]$$

Where s is yearly averaged soil moisture (dimensionless), c is 3, k_l is runoff or leakage at saturation which is 0.1 (yr^{-1}), k_r is the losses regulation rate 0.002 (yr^{-1}), P_o is organic P, P_d is the dissolved P, Zr is soil depth (1m), n is soil porosity (0.4), L_o is the loss rate of P_o and L_d is the loss rate of P_d. Equation 9 in Buendia et al.2010 includes a k_f term or a loss rate from ice, wind, humans, or fire which we do not include because we assume these to be minimal in the Amazon forest prior to the widespread arrival of modern humans. We estimate the steady state ratios of P_o to P_d following figure 2 in Buendia et al. 2010. We estimate the average total loss rate for the Amazon Basin is 0.00007 yr^{-1}. Buendia et al. 2010 calculates a steady state L_d for the Amazon basin of ~3.5 kg km^{-2} yr^{-1} and L_o of ~7 kg km^{-2} yr^{-1}. Our loss rates have a similar ratio of ~2 L_o = L_d. This is an important, yet highly uncertain part of our results and therefore as part of a sensitivity study we double and halve the loss rate. Loss rates of P through occlusion of P are an order of magnitude smaller than loss rates of organic and dissolved P (figure 7 in Buendia et al. 2010) and any uncertainty in occlusion rates will be incorporated within the large range of our sensitivity study.

We estimate the mass of both extinct and extant South American fauna from the Pleistocene and the Holocene based on data from Smith et al.2003 (N=904) [25]. At present it is unknown which extinct megafauna would have lived in the Amazon forest. However, based on limited evidence we are able to make two lists, one of those with animals that "probably" would have ranges that would encompass the current Amazon basin, and one "possibly" could have inhabited the Amazon basin. Based on stable isotope evidence of C3 plant consumption and the location of fossil evidence, we assume that the following species inhabited forest areas of the Amazon: *Eremotherium (3500kg) assume 1 of 2 species),Haplomastodon (6000kg), Cuvieronius (5000kg) assume 1 of 2 species, Toxodon (1100) assume 1 of 4 species, Neochoerus (1500kg) assume 1 of 2 species and Tayassuidae (1100kg) assume 1 of 3 species* [39,40]. Based on a more liberal reading of the evidence, we assume the following species could also have dwelled in the Amazon: *Equus santaelenae, Glossotherium, Holmesina (*Personal communication E. Lindsey and A. Barnosky). Based on the QD equation of $0.05*M^{1.17}$, we calculate a QD value for the Amazon basin of 2.4 km^2 $yr^{-1}$for the "probable" group and 6.5 km^2 $yr^{-1}$for the "possible" group including all species from the "probable" group. In our simulations, we use the midrange value of 4.4 km^2 yr^{-1}, and use 2.4 and 6.5 km^2 yr^{-1} in the sensitivity study. We assume that each of these extinct forest megafauna had a distribution of 100% of the basin based on the abundance of megafauna fossil remains throughout South America and widely dispersed large seeded fruits [41,42].

We display our current estimates of vegetation P with total P and labile P from Quesada et al. 2010 fig 2b [38] (SOM Figure 3). We convert this to Mg km^{-2} for each site using soil bulk density and soil depth provided in the supplementary material (S1 C.A. Quesada) of the paper. We also include data from Fyllas et al. 2009 for leaf P concentrations which we show as vegetation P (Mg km^{-2}) with the assumption of a uniform SLA of 100 g m^{-2} and an LAI of 4 [35]. Where the plots overlap (N=49), we calculate the ratio of vegetation P to labile P and use this to estimate % dust P going into vegetation. Parent material and soil evolutionary stage controls long term (geologic) total P concentrations [38]. Our model does not incorporate these properties and will not replicate current total soil P patterns and concentrations. Instead,

276 our simulations more closely replicate vegetation and labile P patterns because the megafauna increase
277 the readily available form of P that is quickly taken up by the vegetation.

278 We assume a steady state in the absence of animal herbivory of G/K (~50Mg km^{-2}), where G is
279 dust plus local weathering (0.48kg P km^{-2} yr^{-1} plus ~2.5 kg P km^{-2} yr^{-1}) and K is 0.00007 yr^{-1}. We
280 estimate a median labile P of 54 Mg km^{-2} P (SOM Figure 3b) in the Eastern Amazon from Quesada et al.
281 2010 and a median vegetation P of 0.4 Mg km^{-2} P (SOM Figure 3c) from Fyllas et al. (2009). We are
282 interested in the dust P that will enter the vegetation pool, which we estimate as ~1% based on the fact
283 that vegetation P is ~1% of labile P (SOM Figure 3a), and therefore, we apply a multiplication of 0.01 to
284 our dust term.

285

286

287

288

289 *Continental estimates of D*

290 We used the IUCN spatial database on mammal species and their ranges [43] to develop a gridded,
291 global estimate of QD for modern animals[14]. We used this gridded estimate to calculate QD for modern
292 species for continental estimates of Table 1 and for the Amazon basin for Figure 3. We assigned the
293 mean value for the genera or family to species with no body mass data. Edible biomass at 1° resolution
294 was estimated using foliar NPP from the CASA carbon cycle model [44].

295 For extinct species, we use the database from Smith et al. 2003 [25]. Since the ranges of individual
296 species are not currently accurately known, we estimate that at a continental scale each species has a
297 range of ~8% of the continent [45]. We estimate the exact range for each species in the same way as
298 Barnosky (2008) with Africa (8.6%), Australia (7.8%), North America (8.2%), South America (7.2%),
299 and Eurasia (8.1%). This is a highly uncertain term, so we add and subtract 30%, which is incorporated
300 into our uncertainty shown in table 1. There was no data for certain extinct species in Smith et al. 2003
301 for Eurasia and these values were obtained from Barnosky (2008). We assume the percentage of the
302 continent covered in ice during the Pleistocene as: N. America (50%), Eurasia (10%), and S. America
303 (5%) [45].

304

305

306

307 *Possibilities to test predictions*

308 We recognise that we do not yet present any direct evidence that nutrient availability across the
309 Amazonia has declined since the megafaunal extinctions. Instead we have put forward a quantified
310 testable model based on available ecological and geophysical evidence. The collection of direct evidence
311 of nutrient decline following megafaunal loss would require a substantial experimental campaign, and
312 here we propose several potential ways to test our predictions from this study. We would predict a
313 greater quantity of phosphorous flowing out the mouth of the Amazon today than during the era when
314 megafauna still were present in the Amazon basin. We can analyse ocean sediment data from the Ocean
315 Drilling Program (ODP) (http://www-odp.tamu.edu/database/) near the Amazon Fan for changing
316 phosphorous and other nutrient concentrations in a manner similar to which has been done for pollen and
317 isotopes[46].

318 We can look for changes in nutrient concentrations across a nutrient concentration gradient in the
319 presence and exclusion of megafauna. Certain parts of Kruger Park have had all animals >5kg excluded
320 from large regions of the park for 37-43 years and the park has a nutrient concentration gradient due to
321 the granite/basalt substrate. We can compare nutrient gradients both where the animals have been
322 excluded and where they still exist. We predict a diffusion of nutrients across the granite/basalt gradient
323 in the regions with the megafauna, but more of a step change nutrient concentrations in the part of the
324 park without megafauna. This can be tested through airborne analysis of exclusion experiments in Kruger
325 National parks [47].

326 For longer time-scale tests we could compare the sharpness of changes in ecosystem P content
327 (plants, litter and labile soil pools) across sharp geomorphological boundaries (e.g. floodplains vs
328 adjoining terraces), in regions with and without megafauna. In the absence of significant lateral diffusion,
329 ecosystem labile P content should show a step-change across the boundary, reflecting the sharp change in

base substrate. With increasing lateral diffusion, this step change in ecosystem P content becomes increasingly blurred, and the degree of blurring is a direct measure of the diffusivity parameter in our equation. We predict that the measured "blurring" will be much greater in megafauna-rich regions of Africa than in the equivalent geomorphological transitions in Amazonia.

Finally, we can directly test our theory by measuring nutrient concentrations near fertilized farms and forests that are regularly raided by megafauna such as elephants (or experimentally fertilize these areas). We can find out when fertilization of the farm began and how often and by which animals it is raided. From this, we would predict a nutrient gradient into the forest from the fertilized farm. We can test the dung piles as well as the vegetation in the area to determine if the rate of nutrient spread matches that of our predictions.

340

341 **SI Table 1 –** Average P concentrations for leaves, wood, bark, and fruits from Terra firme and blackwater
342 forests and whitewater flood plain forests based on data from Furch and Klinge 1989 (leaves, wood and
343 bark) and Stevenson and Guzman-Caro 2010 (fruit) in units of mg g^{-1} [15,34] (N= number of tree species
344 analysed).

	Leaves mg g^{-1}	Wood mg g^{-1}	Bark mg g^{-1}	Fruit mg g^{-1}
Whitewater flood plain	1.50 (N=88)	0.59 (N=60)	0.80 (N=42)	2.2 (N=10)
Terra Firme and blackwater forests	0.55 (N=220)	0.13 (N=246)	0.16 (N=22)	1.6 (N=13)
Difference	0.95	0.46	0.64	0.4

345

346

347

348 **SI Table 2 -** Table 1. Allometric fits for herbivores >10kg. For the fecal diffusivity fit equation we use

349 all herbivores to increase the sample size.

Dependent Variable	Units	Equation	N	r^2
Population Density	$\#/km^2$	$36.35*M^{-0.58}$	105	0.27
Metabolic Demand	kgDM/#/day	$0.01*M^{0.87}$	24	0.89
Mature Longevity	Days	$5477*M^{0.12}$	116	0.24
Day Range	Km	$0.32*M^{043}$	42	0.41
Home Range	km^2	$0.03*M^{1.19}$	59	0.50
Range Length (√HR)	Km	$0.09*M^{0.59}$	59	0.50
Passage rate*	Days	$0.29*M^{0.28}$	-	-
Fecal Diffusivity, scaling herbivores >10kg	$(kgDM/km^2)*(km^2/day)$	$0.0065*M^{1.41}$	-	-
Fecal Diffusivity, fit all herbivores	$(kgDM/km^2)*(km^2/day)$	$0.05*M^{1.17}$	14	0.67
Bodymass Diffusivity, scaling herbivores >10kg	$(kgDM/km^2)*(km^2/day)$	$6.5*10^{-7}*M^{1.35}$	-	-

350 *equation from Demment and Van Soest et al. 1985 assuming a digestibility of 0.5 [26]

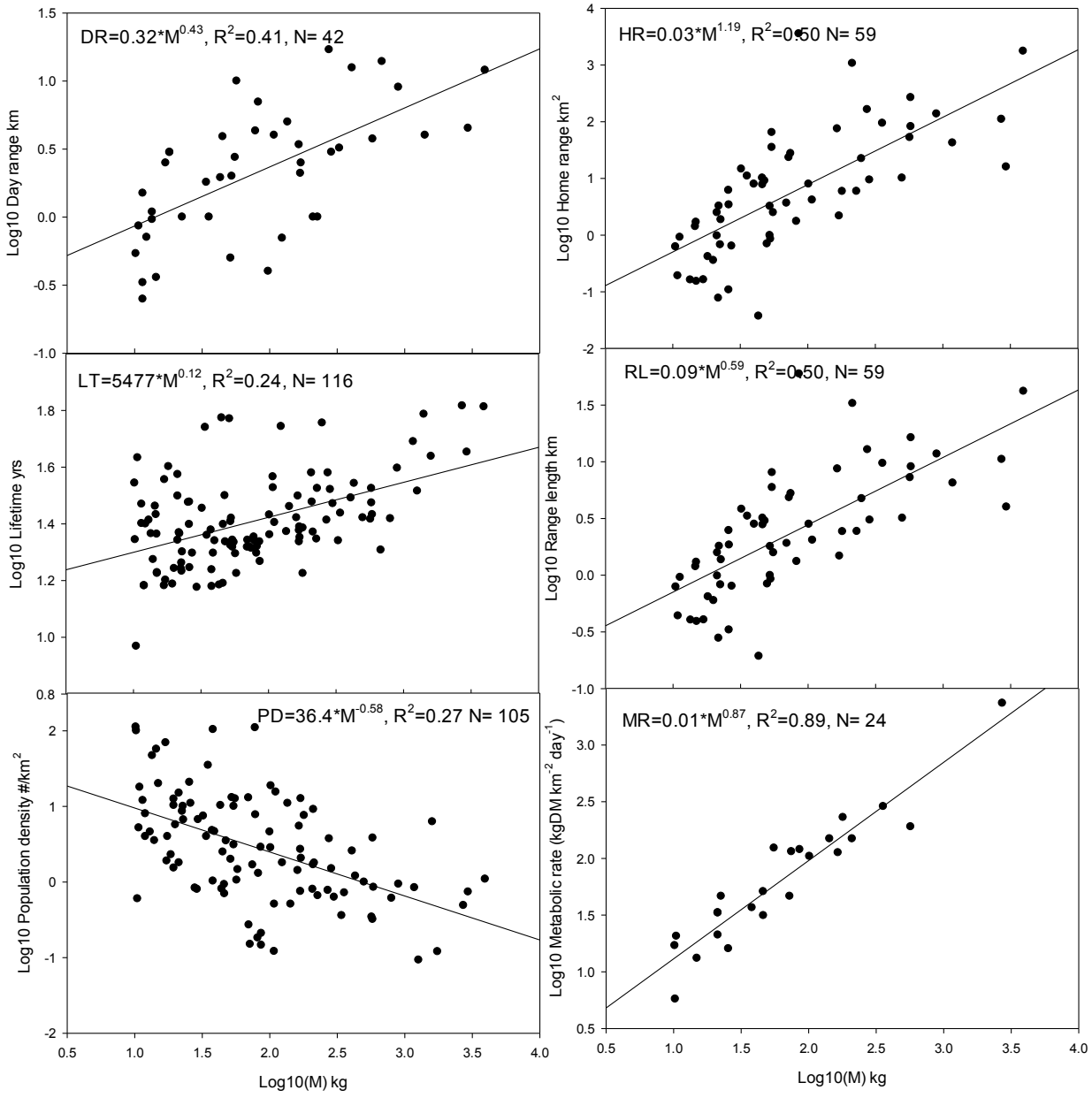

SOM Figure 1 – Log_{10} mass versus log_{10} transformed values of day range (km) (top left), home range (km^2) (top right), lifetime (yrs) (middle right), range length (the square root of home range) (km) (middle left), population density (number of individuals per km^2) (bottom left), and metabolic rate (kg DM km^{-2} day^{-1}) (bottom right) for herbivores >10kg.

357

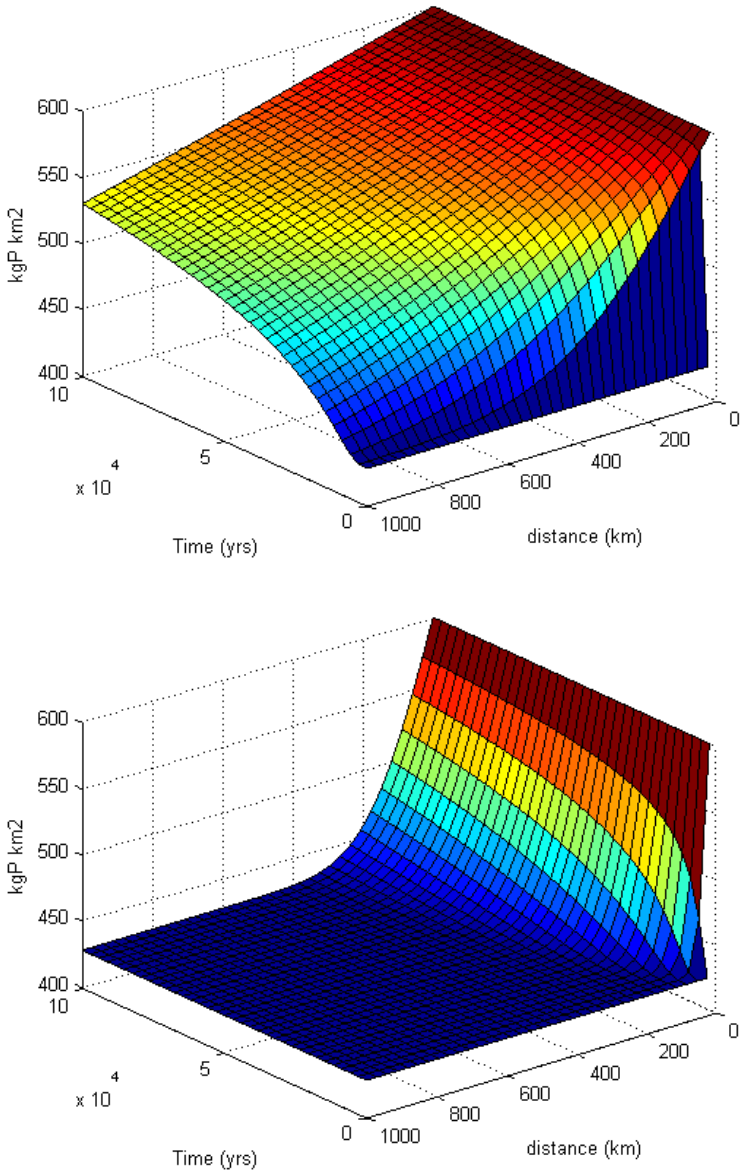

358

359 **SOM Figure 2** – (top) Lateral distribution of nutrients starting from initial conditions over a 1000km

360 distance from a nutrient supply (e.g. the Amazon floodplain) and a 100,000 year period with a $\Phi_{excreta}$

361 value of 4.4 $km^2\ yr^{-1}$(representing lateral diffusion by modern and extinct fauna), (bottom) a $\Phi_{excreta}$ value

362 of 0.027 $km^2\ yr^{-1}$ (representing lateral diffusion by modern fauna only).

363

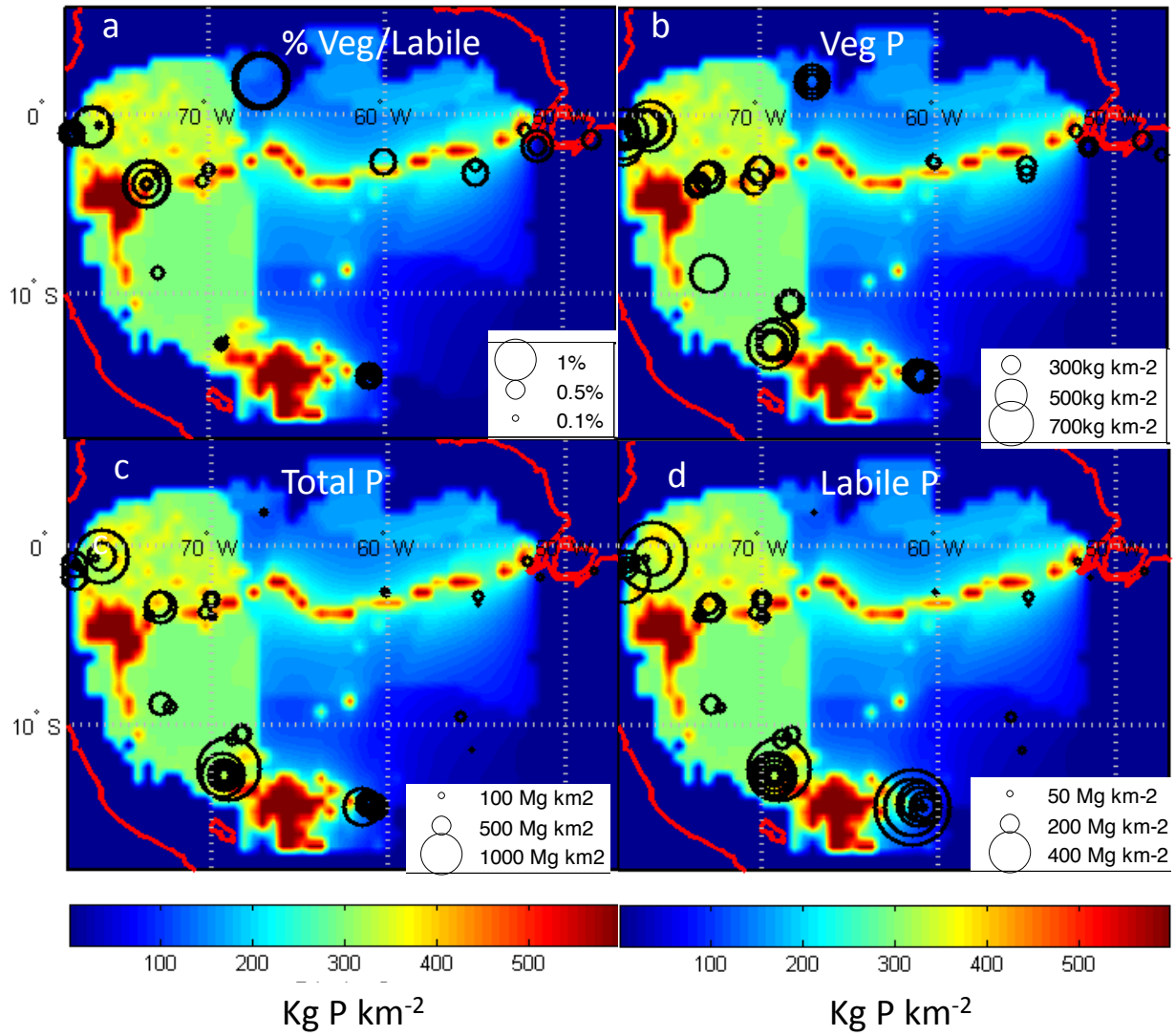

364

365 **SOM Figure 3** – A comparison of our modelled modern-day phosphorus estimates (kg P km^{-2}) (same as

366 Figure 3b) in the background and estimates of (a) percent vegetation/ labile P, (b) vegetation P (kg km^{-2}

367 from Fyllas et al. 2009[35], assuming a SLA of 100g m^{-2} and an LAI of 4), (c) total P (Mg km^{-2}), and (d)

368 labile P (Mg km^{-2}) measured in the Amazon basin from Quesada et al. 2010[38].

369

370

References

1 Okubo, A. & Levin, S. A. *Diffusion and ecological problems : modern perspectives*. 2nd edn, (Springer, 2001).

2 Ovaskainen, O. & Crone, E. E. in *Spatial Ecology Chapman & Hall/CRC Mathematical & Computational Biology* 63-83 (Chapman and Hall/CRC, 2009).

3 Skellam, J. G. Random Dispersal in Theoretical Populations. *Biometrika* **38**, 196-218 (1951).

4 Berg, H. C. *Random Walks in Biology.*, (1993).

5 Ilse, L. M. & Hellgren, E. C. Resource Partitioning in Sympatric Populations of Collared Peccaries and Feral Hogs in Southern Texas. *J Mammal* **76**, 784-799, doi:Doi 10.2307/1382747 (1995).

6 Augustine, D. J. & McNaughton, S. J. Ungulate effects on the functional species composition of plant communities: Herbivore selectivity and plant tolerance. *J Wildlife Manage* **62**, 1165-1183, doi:Doi 10.2307/3801981 (1998).

7 Mcnaughton, S. J. Mineral-Nutrition and Spatial Concentrations of African Ungulates. *Nature* **334**, 343-345, doi:Doi 10.1038/334343a0 (1988).

8 White, K. A. J., Lewis, M. A. & Murray, J. D. A model for wolf-pack territory formation and maintenance. *J Theor Biol* **178**, 29-43 (1996).

9 Frank, D. A., McNaughton, S. J. & Tracy, B. F. The ecology of the Earth's grazing ecosystems. *Bioscience* **48**, 513-521, doi:Doi 10.2307/1313313 (1998).

10 Ellis, J. E. & Swift, D. M. Stability of African Pastoral Ecosystems - Alternate Paradigms and Implications for Development. *J Range Manage* **41**, 450-459, doi:Doi 10.2307/3899515 (1988).

11 Boone, R. B., Coughenour, M. B., Galvin, K. A. & Ellis, J. E. Addressing management questions for Ngorongoro Conservation Area, Tanzania, using the SAVANNA modelling system. *Afr J Ecol* **40**, 138-150 (2002).

12 Bailey, D. W. *et al.* Mechanisms that result in large herbivore grazing distribution patterns. *J Range Manage* **49**, 386-400 (1996).

13 Augustine, D. J., McNaughton, S. J. & Frank, D. A. Feedbacks between soil nutrients and large herbivores in a managed savanna ecosystem. *Ecological Applications* **13**, 1325-1337, doi:Doi 10.1890/02-5283 (2003).

14 Wolf, A., Doughty, C.E., Malhi, Y. Lateral diffusion of nutrients by herbivores in terrestrial ecosystems. *Plos one* (2013).

15 Stevenson, P. R. & Guzman-Caro, D. C. Nutrient Transport Within and Between Habitats Through Seed Dispersal Processes by Woolly Monkeys in North-Western Amazonia. *American Journal of Primatology* **72**, 992-1003, doi:Doi 10.1002/Ajp.20852 (2010).

16 Frank, D. A., Inouye, R. S., Huntly, N., Minshall, G. W. & Anderson, J. E. The Biogeochemistry of a North-Temperate Grassland with Native Ungulates - Nitrogen Dynamics in Yellowstone-National-Park. *Biogeochemistry* **26**, 163-188 (1994).

17 Abbas, F., J. Merlet, N. Morellet, H. Verheyden, A. J. M. Hewison, B. Cargnelutti, J. M. Angibault, D. Picot, J. L. Rames, B. Lourtet, S. Aulagnier, and T. Daufresne. . Roe deer may markedly alter forest nitrogen and phosphorus budgets across Europe. *Oikos* (2012).

18 Rees, P. A. Gross Assimilation Efficiency and Food Passage Time in the African Elephant. *African Journal of Ecology* **20**, 193-198 (1982).

19 Elser, J. J., Dobberfuhl, D.R., MacKay, N.A., Schampel, J.H. Organism Size , Life History, and N:P Stoichiometry. Toward a unified view of cellular and ecosystem processes. *BioScience* **46** (1996).

20 Wilson, D. E. & Reeder, D. M. *Mammal species of the world : a taxonomic and geographic reference*. 3rd edn, (Johns Hopkins University Press, 2005).
21 de Magalhaes, J. P. & Costa, J. A database of vertebrate longevity records and their relation to other life-history traits. *J Evolution Biol* **22**, 1770-1774, doi:DOI 10.1111/j.1420-9101.2009.01783.x (2009).
22 Damuth, J. Interspecific Allometry of Population-Density in Mammals and Other Animals - the Independence of Body-Mass and Population Energy-Use. *Biol J Linn Soc* **31**, 193-246 (1987).
23 Carbone, C., Cowlishaw, G., Isaac, N. J. B. & Rowcliffe, J. M. How far do animals go? Determinants of day range in mammals. *American Naturalist* **165**, 290-297 (2005).
24 Kelt, D. A. & Van Vuren, D. H. The ecology and macroecology of mammalian home range area. *American Naturalist* **157**, 637-645 (2001).
25 Smith, F. A. *et al.* Body mass of late quaternary mammals. *Ecology* **84**, 3403-3403 (2003).
26 Demment, M. W. & Van Soest, P. J. A Nutritional Explanation for Body-Size Patterns of Ruminant and Nonruminant Herbivores. *American Naturalist* **125**, 641-672 (1985).
27 Hayward, A., Kolasa, J. & Stone, J. R. The scale-dependence of population density-body mass allometry: Statistical artefact or biological mechanism? *Ecological Complexity* **7**, 115-124, doi:DOI 10.1016/j.ecocom.2009.08.005 (2010).
28 Crank, J. *The mathematics of diffusion*. 2d edn, (Clarendon Press, 1975).
29 Mahowald, N. M. *et al.* Impacts of biomass burning emissions and land use change on Amazonian atmospheric phosphorus cycling and deposition. *Global Biogeochemical Cycles* **19**, -, doi:Artn Gb4030 Doi 10.1029/2005gb002541 (2005).

30 Buendia, C., Kleidon, A. & Porporato, A. The role of tectonic uplift, climate, and vegetation in the long-term terrestrial phosphorous cycle. *Biogeosciences* **7**, 2025-2038, doi:DOI 10.5194/bg-7-2025-2010 (2010).
31 Crank, J. & Nicolson, P. A Practical Method for Numerical Evaluation of Solutions of Partial Differential Equations of the Heat-Conduction Type. *Proceedings of the Cambridge Philosophical Society* **43**, 50-67 (1947).
32 Hess, L. L., Melack, J. M., Novo, E. M. L. M., Barbosa, C. C. F. & Gastil, M. Dual-season mapping of wetland inundation and vegetation for the central Amazon basin. *Remote Sensing of Environment* **87**, 404-428, doi:DOI 10.1016/j.rse.2003.04.001 (2003).
33 Mcclain, M. E. & Naiman, R. J. Andean influences on the biogeochemistry and ecology of the Amazon River. *Bioscience* **58**, 325-338, doi:Doi 10.1641/B580408 (2008).
34 Furch, K., Klinge, H. Chemical relationships between vegetation, soil and water in contrasting inundation areas of Amazonia. *SPEC. PUBL. BR. ECOL. SOC.* . , 189-204. (1989.).
35 Fyllas, N. M. *et al.* Basin-wide variations in foliar properties of Amazonian forest: phylogeny, soils and climate. *Biogeosciences* **6**, 2677-2708 (2009).
36 Higgins, M. A. *et al.* Geological control of floristic composition in Amazonian forests. *Journal of Biogeography* **38**, 2136-2149, doi:DOI 10.1111/j.1365-2699.2011.02585.x (2011).
37 Richey, J. E. & Victoria, R. L. in *Interactions of C, N, P, and S Biogeochemical Cycles and Global Change.* (ed Mackenzie FT Wollast R, Chou L) 123-140 (Springer, 1993).
38 Quesada, C. A. *et al.* Variations in chemical and physical properties of Amazon forest soils in relation to their genesis. *Biogeosciences* **7**, 1515-1541, doi:DOI 10.5194/bg-7-1515-2010 (2010).
39 MacFadden, B. J. Diet and habitat of toxodont megaherbivores (Mammalia, Notoungulata) from the late Quaternary of South and Central America. *Quaternary Res* **64**, 113-124, doi:DOI 10.1016/j.yqres.2005.05.003 (2005).

40 Sanchez, B., Prado, J. L. & Alberdi, M. T. Feeding ecology, dispersal, and extinction of south American pleistocene gomphotheres (Gomphotheriidae, Proboscidea). *Paleobiology* **30**, 146-161 (2004).
41 Janzen, D. H. & Martin, P. S. Neotropical Anachronisms - the Fruits the Gomphotheres Ate. *Science* **215**, 19-27 (1982).
42 Do Nascimento, W. M. O., De Carvalho, J. E. U. & Muller, C. H. Occurrence and geographical distribution of bacuri. *Revista Brasileira De Fruticultura* **29**, 657-660 (2007).
43 IUCN. (2010).
44 Field, C. B., Behrenfeld, M. J., Randerson, J. T. & Falkowski, P. Primary production of the biosphere: Integrating terrestrial and oceanic components. *Science* **281**, 237-240 (1998).
45 Barnosky, A. D. Megafauna biomass tradeoff as a driver of Quaternary and future extinctions. *Proceedings of the National Academy of Sciences of the United States of America* **105**, 11543-11548, doi:DOI 10.1073/pnas.0801918105 (2008).
46 Maslin, M. A., Ettwein, V. J., Boot, C. S., Bendle, J. & Pancost, R. D. Amazon Fan biomarker evidence against the Pleistocene rainforest refuge hypothesis? *Journal of Quaternary Science* **27**, 451-460, doi:Doi 10.1002/Jqs.1567 (2012).
47 Asner, G. P. & Levick, S. R. Landscape-scale effects of herbivores on treefall in African savannas. *Ecology Letters* **15**, 1211-1217, doi:DOI 10.1111/j.1461-0248.2012.01842.x (2012).